System-level reliability assessment for a direct-drive PMSG based wind turbine with multiple converters

Ye, Shuaichen; Zhou, Dao; Blaabjerg, Frede

Published in:
Microelectronics Reliability

DOI (link to publication from Publisher):
10.1016/j.microrel.2020.113801

Publication date:
2020

System-level Reliability Assessment for a Direct-drive PMSG Based Wind Turbine with Multiple Converters

Shuaichen Ye[a], Dao Zhou[b*], Frede Blaabjerg[b]

[a] *School of Aerospace Engineering, Beijing Institute of Technology, Beijing, China*
[b] *Department of Energy Technology, Aalborg University, Aalborg, Denmark*

Abstract

System-level reliability of the wind power converter has an essential effect on the operation performance and lifespan of a wind turbine system. In this paper, a wind turbine equipped with a 2 MW direct-drive permanent-magnet synchronous generator (PMSG) serves as a case study. Considering the maximum stator current limitation of the PMSG, several multiple-converter structures and their reliability block diagrams (RBDs) are constructed for the machine side converter (MSC). To investigate the reliability influence caused by the amount of semiconductor components and the current for each component, the structures with four and five bridges in parallel are both configured. Reliability evaluation between two major parallel structures, namely, bridges in parallel and converters in parallel are also compared. In addition, the effect of different wind classes on the MSC system-level reliability has also been investigated. A detailed discussion regarding the system reliability cumulative distribution function (CDF) is presented, which could serve as reference for future MSC structure design. It is concluded that the component current dominates in the system-level reliability of the MSC and the standby structure can also improve the reliability under the same current level. Besides, compared with the different converter structures, various wind classes have a minor impact on the system-level reliability.

Keywords: System-level reliability; wind turbine; permanent-magnet synchronous generator (PMSG); machine side converter (MSC); bridges in parallel; converters in parallel; wind class

1. Introduction

Conventionally, the doubly-fed induction generator (DFIG)-based partial-scale power converter structure is regarded as a mainstream candidate for the wind power generation system, because of its low power burden for the machine side converter (MSC) [1]. However, with the upgrade and development of the grid codes, a stricter grid environment emerges [2], which brings the difficulty in low-voltage ride-through for the traditional partial-scale converter structure [3,4]. To solve this issue, the permanent-magnet synchronous generator (PMSG)-based full-scale power converter is selected as an alternative. The full-scale MSC carries all the power generated by the PMSG, which indicates that, in the case of the identical power converter design, the failure rate of the full-scale MSC might be much higher than that of the partial-scale MSC. Therefore, the reliability of the full-scale MSC should be investigated in a precise manner. Meanwhile, in recent decades, the wind farm is moving from onshore to some rugged offshore environments for a better wind condition, which increases the maintenance cost of the turbine equipment [5]. Consequently, a system-level reliability assessment for wind turbines is essential in their design process.

Fig. 1 shows a typical direct-drive PMSG based wind power generation system, which includes the subsystems of a turbine, a generator, converters and control circuits, transformers and grid. Among them, the converter module is regarded as one of the most fragile components [5]. Therefore, the reliability of the entire system can largely be revealed by the characteristic of the power converter. This paper mainly focuses on the reliability assessment of the MSC, and the method can also be applied to the investigation of the grid side converter (GSC).

Primary research of assessing the reliability of the power converter focused on calculating the B_X lifetime (the failure rate of a product is X% at this operational moment) of the semiconductors (diode and IGBT) [6]. However, these results can only reflect the reliability of the semiconductors from a certain aspect rather than from the entire tendency. Based on the B_X lifetime calculation, the Bayerer's model and the Monte Carlo method are applied to generate the reliability cumulative distribution function (CDF) for

* Corresponding author. zda@et.aau.dk

semiconductors [7]. Moreover, the reliability of one converter with six IGBTs and six diodes can subsequently be obtained by multiplying the reliability CDFs of all semiconductors. Although the converter-level reliability can directly be assessed according to existing literatures, for the high-power large-current PMSG, single converter is insufficient. Thus, some structures like converters and bridges in parallel need to be applied to distribute the current burden of each power component. However, researches which consider system-level reliability for multiple-converter structures are still lacking.

This paper takes a PMSG wind turbine with the specification of 2 MW/3.5 kA as the case study, and uses common low-voltage semiconductors with the rating of 1 kA/1.7 kV as basic units in the MSC. Considering the maximum PMSG stator current, several feasible structures like bridges in parallel and converters in parallel structures are designed for the MSC, their system-level reliability CDF comparisons are obtained based on their reliability block diagrams (RBDs) and reliability calculation formulas. Detailed results and discussions are presented combing with the practical MSC working circumstances and different wind classes. The contribution of this paper is to provide some suggestions for the structure design process of the MSC.

2. Calculation process from mission profile based component reliability to converter reliability

Before the calculation of the system-level reliability, the reliability of single converter should be assessed based on the semiconductor components, namely, the diode and the IGBT. A mission profile based component reliability to converter reliability calculation flowchart from the component to the converter is shown in Fig. 2 [6].

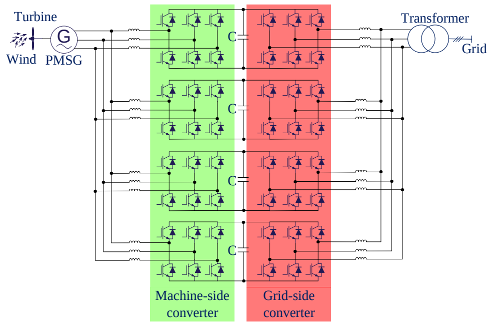

Fig. 1. Configuration of a direct-drive PMSG based wind power generation system.

In this calculation, a 1-year wind speed distribution is regarded as the basic mission profile, the semiconductor lifetime under long-term thermal cycle (long-term thermal cycle uses real-time annual wind-speed as the mission profile, the cycle period is from several minutes to one hour) and short-term thermal cycle (short-term thermal cycle uses annual wind speed Weibull distribution as the mission profile, and its cycle frequency is related to the PMSG stator current frequency, which is from several to dozens of Hz) are included. The long-term thermal cycle based lifetime of diode and IGBT can be obtained via the turbine model, the PMSG model, the converter model, the loss model, the thermal model, the Rainflow counting algorithm and the Coffin-Manson lifetime model. On the other hand, the short-term thermal cycle based semiconductor lifetime can be obtained using the 1-year wind speed Weibull distribution via a similar process without the Rainflow counting algorithm. It is worthwhile to note that, in

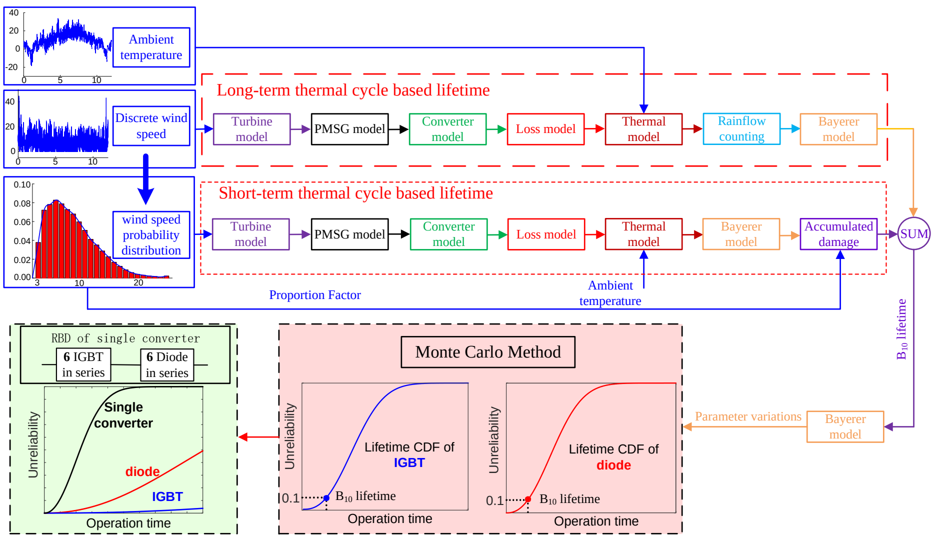

Fig. 2. Calculation flowchart from mission profile based component reliability to the converter reliability.

the thermal model, besides the temperature rise due to the loss dissipation of components, the ambient temperature should also be considered and added to obtain the chip junction temperature. After summing of the short-term and long-term thermal cycle based component lifetime, the B_{10} lifetime of the diode and the IGBT are estimated. Using a Bayerer's model and considering its coefficients with 5% variations from their average values, normal distributions of these coefficients are generated. Considering all coefficient variations, a Monte Carlo method is used to simulate the lifetime probability distribution functions (PDFs) of the diode and the IGBT according to the Weibull distribution, and the reliability (or unreliability) CDFs of the diode and the IGBT can be subsequently calculated. Finally, the RBD of one converter is constructed as six IGBTs and six diodes in series, leading to system-level reliability calculated by multiplying the reliabilities of all these twelve components.

3. Bridges in parallel structure (Case 1) and corresponding system-level reliability

Bridges in parallel structure is one of the methods that can distribute the current burden for each semiconductor in the converter. This method connects several semiconductors of the same kind to one joint point. It is assumed that, due to the common gate driver for various semiconductors in one bridge, the failure of one semiconductor leads to the failure of the entire converter system. In this paper, the bridges in parallel structure is considered as Case 1. As described above, the rated current of the PMSG is 3.5 kA and the rated current for the power modules used in each MSC leg is 1 kA, which means that the minimum amount of the bridge is four.

Two cases are investigated for bridges in parallel structure. Case 1-1 has four bridges in parallel, which includes 24 diodes and 24 IGBTs in total. This case is the situation with the minimal components, and can be regarded as four bridges are connected to one MSC leg. It is noted that the current for each semiconductor during on-state is $I_s/4$ (I_s is the PMSG stator current). Case 1-2 has five bridges in parallel, which indicates amounts of the diode and the IGBT are both 30, and the loading current for each semiconductor becomes $I_s/5$. The structure diagrams and RBDs for Case 1-1 and Case 1-2 are shown as Fig. 3 and Fig. 4, respectively.

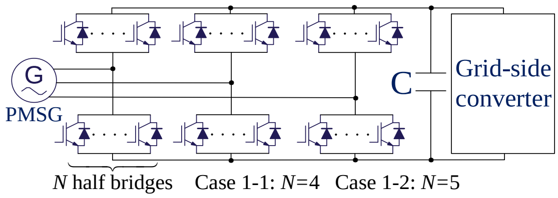

Fig. 3. Configuration for four bridges in parallel (Case 1-1) and five bridges in parallel (Case 1-2).

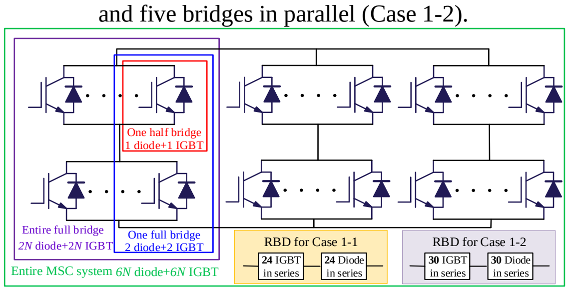

Fig. 4. Reliability block diagram for four bridges in parallel (Case 1-1) and five bridges in parallel (Case 1-2).

Consequently, based on RBDs and the fatigue mechanism that one semiconductor failure causes the failure of the entire converter, the unreliability calculation for Case 1-1 and Case 1-2 can be deduced as Eq. (1) and (2), respectively.

$$F^{(4)}_{\text{bridges in parallel}} = 1-(1-F^{(4)}_T)^{24} \times (1-F^{(4)}_D)^{24} \tag{1}$$

$$F^{(5)}_{\text{bridges in parallel}} = 1-(1-F^{(5)}_T)^{30} \times (1-F^{(5)}_D)^{30} \tag{2}$$

wherein $F^{(n)}_T$ and $F^{(n)}_D$ denote the unreliability of single IGBT and single diode, respectively, in the case of n bridges in parallel. Based on the flowchart in Fig. 2 and calculation formulas, unreliability of the entire MSC and each components of Case 1-1 and 1-2 are illustrated in Fig. 5 and Fig. 6, respectively.

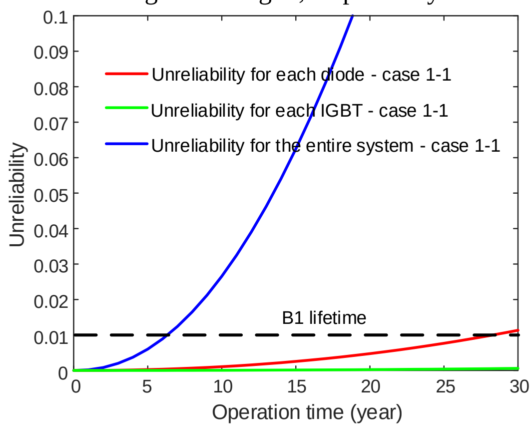

Fig. 5. Unreliability for single diode, single IGBT and the entire converter in Case 1-1: Four bridges in parallel.

From Case 1-1 to Case 1-2, it can be seen that the total amount of the power semiconductors increases, which reduces their current during the on-state period. According to the PMSG model and the converter model in Fig. 2, a smaller current results in a lower junction temperature and a higher reliability for a single power component. However, with the increasing amount of the semiconductors, the failure rate for the entire system may also increase.

Therefore, a trade-off between the semiconductor current and the amount of the components needs to be investigated. Compared with results in Fig. 5 and Fig. 6, although Case 1-2 has a larger amount of power devices, its reliability value at the same operation period and the B_1 lifetime are still higher than that in Case 1-1, which indicates that the current loading has a more significant impact on the reliability of the system instead of the semiconductor amount.

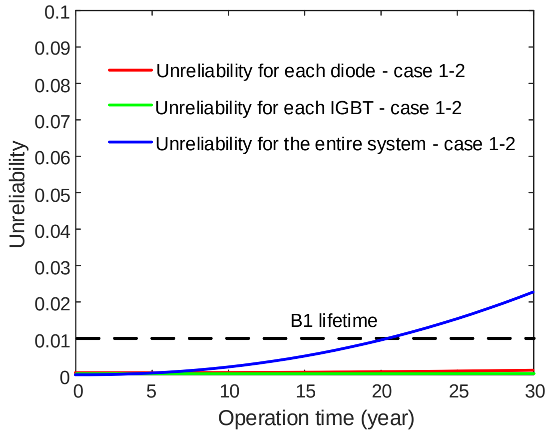

Fig. 6. Unreliability for single diode, single IGBT and the entire converter in Case 1-2: Five bridges in parallel.

4. Converters in parallel structure (Case 2) and corresponding system-level reliability

Converters in parallel structure is another approach to share the total loading current, which considers a converter with six diodes and six IGBTs as a basic unit. In this section, the situation with five converters in total is considered as Case 2, which has 30 diodes and 30 IGBTs in total. According to the rated current from the generator stator, the minimum amount of the converter is four, and four converters in parallel structure has a same reliability assessment with Case 1-1: Four bridges in parallel. Moreover, the method used in this section can also be expanded to the situation with more than 5 converters in parallel structures.

4.1. Case 2-1: Five converters in parallel structure without a standby converter

The structure and RBD of Case 2-1 are shown in Fig. 7(a), and its working principle is explained as follows. In the initial period, five converters work together, the current for each component is $I_s/5$. When one converter fails, the system turns to four converters in parallel structure, and the current for each component becomes $I_s/4$. Consequently, according to the working principle, the unreliability calculation formula of Case 2-1 is written as follows [8]:

$$F_{\text{nostandby}}^{(5)} = (1 - F_{\text{bridges in parallel}}^{(5)}) + (1 - F_{\text{bridges in parallel}}^{(4)}) - (1 - F_{\text{bridges in parallel}}^{(5)}) \times (1 - F_{\text{bridges in parallel}}^{(4)})$$

(3)

4.2. Case 2-2: Five converters in parallel structure with a standby converter

The structure and RBD of Case 2-2 are presented in Fig. 7(b). Its working principle is in the initial period, four active converters operate together, and current for each component is $I_s/4$. In the case that one converter fails, the standby converter starts to take over and work together with the other three remaining converters, and the current for each component is still $I_s/4$.

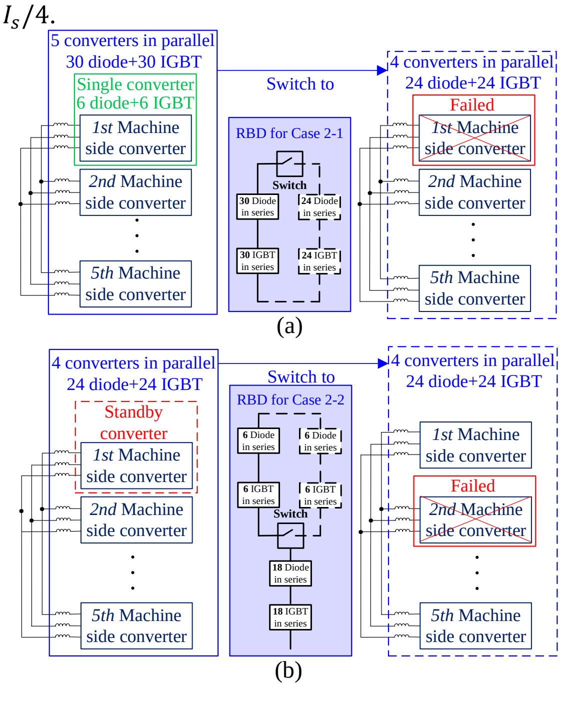

Fig. 7. Configurations and reliability block diagrams for (a) Five converters in parallel structure without a standby converter (Case 2-1), and (b) Five converters in parallel structure with a standby converter (Case 2-2).

Then, the unreliability calculation formula of this case can be derived based on Fig. 7(b) as follows:

$$F_{\text{withstandby}}^{(5)} = 1-(1-F_T^{(4)})^{18}\times(1-F_D^{(4)})^{18}\times[(1-F_T^{(4)})^{6}\times(1-F_D^{(4)})^{6} +(1-F_T^{(4)})^{6}\times(1-F_D^{(4)})^{6}-(1-F_T^{(4)})^{12}\times(1-F_D^{(4)})^{12}] \quad (4)$$

4.3. Comparisons between Case 2-1 and Case 2-2

Combing the fundamental calculations in Case 1, the unreliability for Case 2-1 and Case 2-2 can be obtained by Eq. (3) and Eq. (4), respectively, and their comparisons are shown in Fig. 8.

From Fig. 8, it is observed that the case without a standby has an obvious higher reliability than the case with a standby converter, because for the operation period without failed converter, the current of the semiconductor in Case 2-1 ($I_S/5$) is much lower than that in Case 2-2 ($I_S/4$).

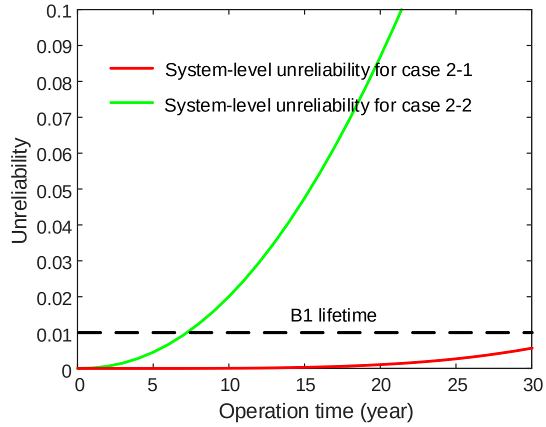

Fig. 8. System-level unreliability for five converters in parallel structure without a standby converter (Case 2-1), and five converters in parallel structure with a standby converter (Case 2-2).

This result also indicates the current takes a very major effect to the reliability of the system, and this effect may even eliminate the superiority of a standby redundancy.

5. Comparison between bridges in parallel (Case 1) and converters in parallel (Case 2)

As the component current for Case 1-1 and Case 2-2 are both $I_S/4$, a comparison of the system-level reliability between these two cases is shown in Fig. 9. From Fig. 9, reliability of Case 2-2 is higher than that of Case 1-1 in the entire operation range. It is obvious that this reliability improvement owes to the introduction of a standby converter. Combing with the results in Fig. 8, it indicates that although the standby redundancy has a minor effect to the system-level reliability comparing with the current reducing, it still upgrades the reliability under the same current level.

For Case 1-2 and Case 2-1, their component currents are both $I_S/5$ in the initial operation period. A system-level reliability comparison between these two methods is presented in Fig. 10, which shows that the reliability of Case 2-1 is a much larger than that of Case 1-2. This is because Case 1-2 operates at the current of $I_S/5$ for the entire operation range, and can switch to four converters in parallel structure if one converter fails in its initial five converters in parallel structure. Thus, for a short-term operation, a converter breakdown in both of Case 1-2 and Case 2-1 may be caused by an external random reason and the four remaining converters in Case 2-1 can still operate for a longer period, which is the reason Case 2-1 has a higher reliability than Case 1-2.

6. Influence of different wind classes on the MSC system-level reliability

According the wind turbine design standard provided by IEC [9], there are three kinds of typical wind class, namely, Class I, Class II and Class III, where average wind speed is 7.5 m/s, 8.5m/s and 10 m/s, respectively.

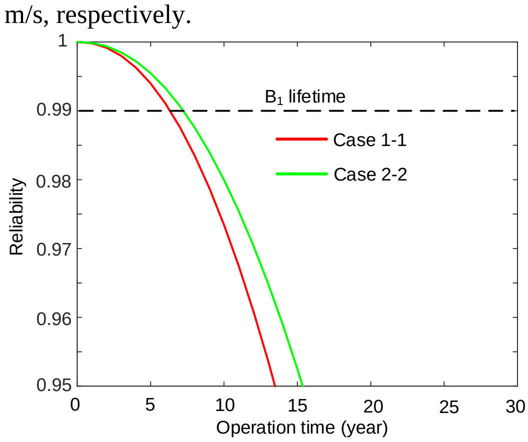

Fig. 9. System-level reliability comparison between four bridges in parallel (Case 1-1) and five converters in parallel structure with a standby converter (Case 2-2).

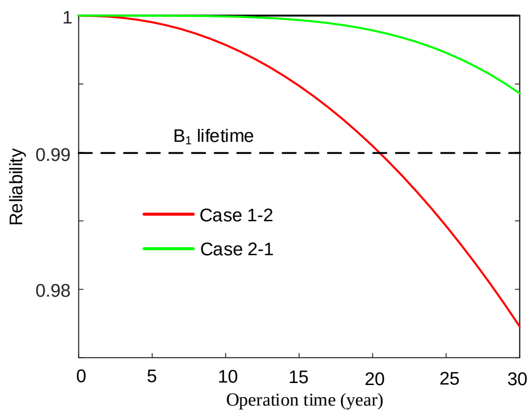

Fig. 10. System-level reliability comparisons between five bridges in parallel (Case 1-2) and five converters in parallel structure without a standby converter (Case 2-1).

Expressing these three wind classes by the Weibull distribution [10]:

$$f(v) = \frac{k}{A}\left(\frac{v}{A}\right)^{k-1} e^{\left(-(v/A)^k\right)} \quad (5)$$

wherein, A is the Weibull scale parameter in m/s, which is proportional to the mean wind speed, and k is the Weibull scale parameter. For different wind classes, parameters are fitted as, in Class I, A=8.61 k=1.79, in Class II, A=9.65 k=1.99 and in Class III, A=11.26 k=2.32, and their PDFs are illustrated as Fig. 11.

Then, by using the calculation process in Section 2, and apply these three wind classes to Case 1-1 (four bridges in parallel) of the MSC, system unreliability profiles can be obtained via Eq. (1) and are illustrated in Fig. 12. It is observed that although various wind classes induce different system-level reliabilities of the MSC, the influence is still minor compared with the system configuration changing. It is deduced that this minor influence mainly produced by the mean wind speed variation.

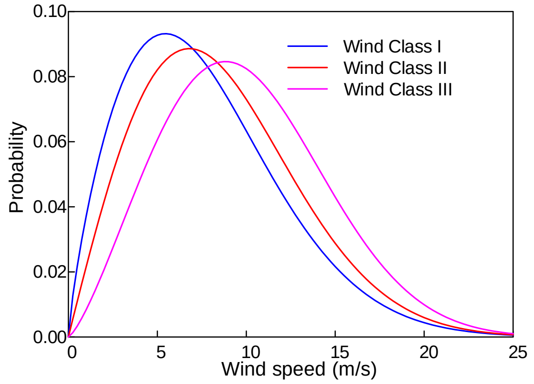

Fig. 11. Wind speed probability distribution functions for Class I, Class II and Class III under Weibull distribution.

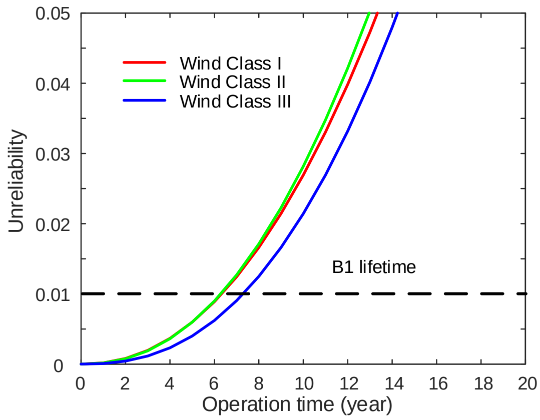

Fig. 12. System-level unreliability for four bridges in parallel (Case 1-1) under different wind classes.

6. Conclusions

This paper designs several bridges in parallel and converters in parallel structures of the MSC for a 2 MW PMSG based wind turbine considering the rating of the power device. The RBDs, the system-level reliability calculation formulas and reliability (or unreliability) profiles of all cases are given. It is found that among all the cases, Case 2-1: five converters without a standby, which has 30 diodes and 30 IGBTs in total, reaches the highest reliability from the B_1 lifetime point of view. Furthermore, comparative results show that compared with the component amount and the standby redundancy, the current for each component takes a more effect to the system-level reliability, and the standby redundancy can only improve the reliability finitely under the same current level. Moreover, different wind classes have minor influence to the system-level reliability compared with the various converter configuration. Therefore, when designing an MSC with several converters, the most preferred strategy of upgrading the reliability is to reduce the current for each component. Then, a tradeoff between the standby redundancy, the cost and the localized wind class should be considered.

References

[1] J. Manwell, J. McGowan, A.L. Rogers, Wind Energy Explained: Theory, Design and Application, John Wiley & Sons, 2010.

[2] M. Tsili and S. Papathanassiou, “A review of grid code technical requirements for wind farms,” *IET Renew. Power Gener.*, vol. 3, no. 3, pp. 308–332, Sep. 2009.

[3] S. Xiao, G. Yang, H. Zhou, and H. Geng, “An LVRT control strategy based on flux linkage tracking for DFIG-based WECS,” *IEEE Trans. Ind. Electron.*, vol. 60, no. 7, pp. 2820–2832, Jul. 2013.

[4] J. Lopez, E. Gubia, E. Olea, J. Ruiz, and L. Marroyo, “Ride through of wind turbines with doubly fed induction generator under symmetrical voltage dips,” *IEEE Trans. Ind. Electron.*, vol. 56, no. 10, pp. 4246–4254, Oct. 2009.

[5] B. Hahn, M. Durstewitz, and K. Rohrig, “Reliability of wind turbines-Experience of 15 years with 1500 WTs,” in Wind Energy: Proceedings of the Euromech Colloquium. Berlin, Germany: Springer-Verlag, pp. 329–332.

[6] D. Zhou, F. Blaabjerg, M. Lau, and M. Tonnes, “Comparison of wind power converter reliability with low-speed and medium-speed permanent-magnet synchronous generators,” *IEEE Trans. on Ind. Electron.*, vol. 62, no. 10, pp. 6575-6584, Oct. 2015.

[7] D. Zhou, G. Zhang, and F. Blaabjerg, “Optimal selection of power converter in DFIG wind turbine with enhanced system-level eeliability,” *IEEE Trans. on Ind. Appl.*, vol. 54, no. 4, Jul./Aug. 2018.

[8] P. D. T. O’Connor and A. Kleyner, Practical Reliability Engineering, 5thed. New York, NY, USA: Wiley, 2012.

[9] Wind turbines—Part I: Design requirements, IEC 61400-1, 3rd ed., 2005.

[10] Swiss wind power data website. [Online]. Available: http://wind-data.ch/tools/weibull.php.